BSA-Mediated Stabilized Dispersion of Hydrophobic Organic Nanoparticles Produced by Pulsed Laser Fragmentation in Liquid

Akiko Sunada[1], Tomosumi Kamimura[2,3], and Ryohei Yasukuni[*2]

[1]*Division of Electrical, Electronics and Mechanical Engineering, Graduate School of Engineering, Osaka Institute of Technology, 5-16-1 Ohmiya, Asahi-ku, Osaka, 535-8585, Japan*
[2]*Department of Electronics and Information Systems Engineering, Faculty of Engineering, Osaka Institute of Technology, 5-16-1 Ohmiya, Asahi-ku, Osaka, 535-8585, Japan*
[3]*Institute of Laser Engineering, The University of Osaka, 2-6 Yamadaoka, Suita, Osaka 565-0871, Japan*
**Corresponding author's e-mail: ryohei.yasukuni@oit.ac.jp*

The complex synthesis of nanopharmaceuticals still faces hurdles regarding stability, sterilization, storage, and quality control toward industrial production of poorly water-soluble drug formulations. In this study, we investigated the versatility of bovine serum albumin (BSA) as a biocompatible dispersing agent for nanoparticles produced by Pulsed Laser Fragmentation in Liquid (PLFL). We selected quinacridone (QA) as a model compound of nanomedicine due to its low topological polar surface area (tPSA = 58.2 Å²), representing a higher degree of hydrophobicity that typically face solubility problem in gastrointestinal fluids. PLFL of QA in BSA solution yielded finer nanoparticles with enhanced fragmentation efficiency compared to those in water. While QA nanoparticles produced in water agglomerated immediately in phosphate-buffered saline (PBS), nanoparticles exhibited long-term dispersion stability in the presence of BSA. Furthermore, fluorescence spectroscopy revealed molecular-like emission bands only with BSA, suggesting that strong hydrophobic interactions disturbed the surface molecular arrangement. These results demonstrate that BSA can serve an effective dispersing agent for low tPSA compounds.

DOI:10.2961/jlmn.2026.02.2009

Keywords: Pulsed Laser Fragmentation in Liquid, Nanopharmaceuticals, Organic nanoparticles, Bovine serum albumin, Dispersion stability

1. Introduction

Advances in synthetic technology over the last three decades have increased the prevalence of poorly soluble drugs with complex molecular structures. According to the Biopharmaceutics Classification System (BCS), approximately 40% of currently marketed oral medications are classified as poorly water-soluble (BCS Classes II and IV) [1]. Consequently, enhancing the solubility of these compounds remains a critical challenge in pharmaceutical development [2].

Nanopharmaceuticals, which encapsulate drug compounds into nanoscale formulations, have garnered significant attention due to their potential to substantially enhance solubility and improve *in vivo* pharmacokinetics [3]. However, the complex synthesis of nanomedicines still faces hurdles regarding stability, sterilization, storage, and quality control toward industrial production [4].

Pulsed Laser Fragmentation in Liquid (PLFL) has been successfully used to fabricate a variety of organic nanoparticles [5-7]. In this technique, bulk crystals suspended in a liquid medium are exposed to laser pulses. The rapid temperature increase induces volume expansion, leading to the fragmentation of the bulk crystals into nanoparticles. A key advantage of PLFL is the direct production of colloidal nanoparticle suspensions in water without the need for organic solvents or dispersing agents. Furthermore, the simplicity of the procedure facilitates quality control for industrial-scale manufacturing, making PLFL a promising technique for nanomedicine production. Nevertheless, once these nanoparticles are introduced into physiological solutions, they tend to aggregate, which can affect *in vivo* pharmacokinetics.

We previously reported that nanoparticles of Pigment Red 149 (PR149), a perylene compound used as a model for poorly soluble drugs, produced by PLFL in a bovine serum albumin (BSA) solution exhibit high dispersion stability in physiological environments [8]. This study indicated that BSA can interact strongly with insoluble nanoparticles, functioning as a biocompatible dispersing agent. However, it remains unclear whether such interactions are specific to the molecular structure of perylene compounds.

To address this, we focused on Topological Polar Surface Area (tPSA), a key metric for predicting drug solubility and transport. While a tPSA of 70–120 Å² typically ensures balanced solubility for oral medications, values below 60 Å² often lead to solubility problem in gastrointestinal fluids [9].

In this study, quinacridone (QA) was selected as a model compound to test the BSA-mediated stabilization in

physiological environments. With a tPSA of 58.2 Å², QA is more hydrophobic than PR149 (74.76 Å²). We investigated whether BSA can effectively stabilize QA nanoparticles despite their lower tPSA and distinct molecular structure [9].

2. Experimental Procedures

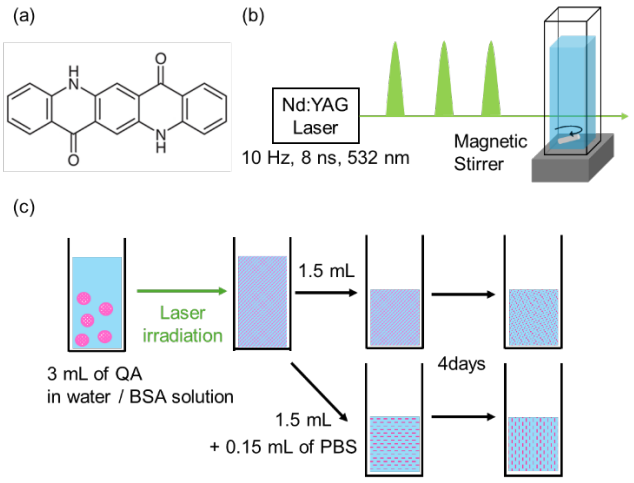

Fig.1 (a) Molecular structure of QA. (b) Schematic illustration of the laser irradiation system for PLFL. (c) Summary of experimental procedures

QA was purchased from Tokyo Chemical Industry Co., Ltd. and used without further purifications as a model compound of poorly soluble drugs. The molecular structure of QA is shown in Fig. 1(a). Bovine serum albumin (BSA, Nacalai tesque)), a protein with a molecular weight of 66.5 kDa and a Stokes radius of approximately 3.5 nm, was used as a dispersing agent.

QA powder was first suspended in ultrapure water and subjected to ultrasonication for 5 min, followed by mixing with either deionized water or an aqueous BSA solution (4 mg/mL) to prepare suspensions with a final QA concentration of 0.003 wt%.

The PLFL system is shown in Fig. 1(b). 3.0 mL of the sample suspension was placed in a quartz cuvette (1 x 1 x 5 cm3) and then exposed to the frequency-doubled beam of a nanosecond yttrium aluminum garnet (YAG) laser (Continuum, Surelite II) at an energy density of 20 mJ/cm² for 15 min with vigorous stirring. The diameter of the laser spot was 5 mm.

UV-VIS absorption spectra were measured using a tungsten halogen lamp (Thorlabs, SLS201L) as a white light source and a multi-channel fiber spectrometer (StellarNet Inc., EPP2000).

The size distribution and the zeta potential of the NPs were determined by dynamic light scattering and laser doppler analysis respectively (Horiba, nanoPartica SZ-100). Three measurements were made for each sample and the average was taken. A viscosity of 0.89 cP for water and 1.3 cP for BSA solution was used to calculate the size of NPs.

Fluorescence spectra were measured with fluorescence spectrometer (Acton Research, SpectraPro 500i) coupled with a CCD detector (Princeton Instruments, PIXIS100B) at 473 nm excitation at 50 mW.

To assess dispersion stability, Dulbecco's phosphate-buffered saline (pH 7.2-7.8, PromoCell GmbH) was employed. PBS was selected because it is a balanced salt solution widely used in tissue culture to mimic physiologically relevant conditions, including osmotic balance and pH. Following laser irradiation, the suspension was divided into 2 aliquots of 1.5 mL, and PBS was added to one of the aliquots. Absorption spectra and particle size distributions were then measured after laser irradiation and 4 days after PBS addition. The overview of the experimental procedure is summarized in Fig. 1(c).

3. Results and Discussion

The QA compound exhibited poor solubility in water, with its initial bulk crystals (> 1 μm) either settling at the bottom or floating within the cuvette prior to laser irradiation. Figure 2(a) shows the laser-induced changes in the absorption spectrum. Before irradiation, the spectrum showed two absorption peaks at 530 nm and 560 nm.

Following exposure to laser pulses at 20 mJ/cm² for 15 minutes, the suspension became a transparent magenta solution. The two absorption peaks increased, while the absorbance above 600 nm decreased.

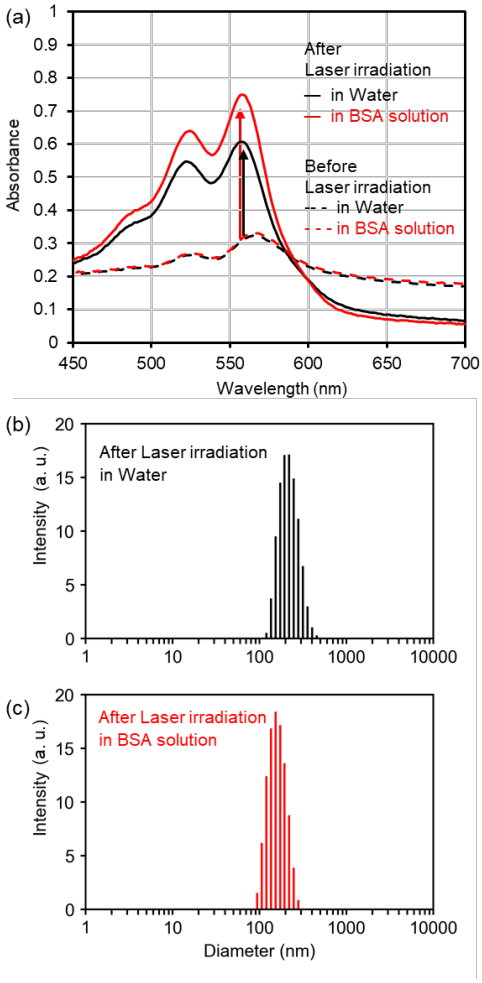

Fig. 2 (a) UV-vis absorption spectra of QA suspended in water (black) and in BSA solution (red) before (dashed lines) and after (solid lines) laser irradiation. (b, c) Particle size distributions of QA nanoparticles produced by laser irradiation (b) in water and (c) in BSA solution.

This spectral change is attributed to the laser-induced fragmentation of the bulk QA crystals and the subsequent formation of nanoparticles [10]. The initial crystals were significantly larger than the optical penetration depth (on the order of a few hundred nanometers); thus, light absorption was limited to their surface. Fragmentation increased the total surface area contributing to the increase absorption of QA. Conversely, this reduction in crystal size led to a significant decrease in the Mie scattering contribution, resulting in the observed drop in absorbance in the 600–700 nm range. The formation of QA nanoparticles was also confirmed by DLS measurement. The particle size distribution of QA suspension after laser irradiation was shown in Fig. 2 (b). The mean particle size was 212 nm with poly dispersed index (PDI) of 0.26.

When the bulk QA crystals were suspended in the BSA solution, the absorption spectrum before laser irradiation was nearly identical to that in water. After laser irradiation, larger absorption peaks at 530 nm and 560 nm and the smaller mean particle size of 147 nm with PDI of 0.24 were observed compared to the case in water (Fig.2(a, c)). When BSA solutions (without QA) were subjected to laser irradiation in the same laser conditions, no changes were observed in the absorption spectra or size via DLS, confirming that BSA remains stable and does not form aggregates or side products under PLFL. Therefore, the observed spectrum was attributed solely to QA. These results suggest that nanoparticle formation was enhanced in the presence of BSA.

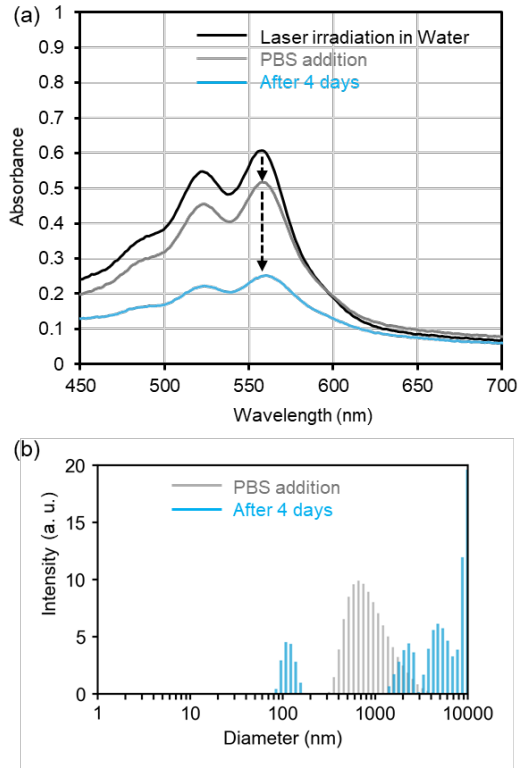

Fig. 3 (a) UV-vis absorption spectra of QA nanoparticles formed in water (black) and immediately after PBS addition (gray) and after 4 days (blue). (b) Particle size distributions of QA nanoparticles after PBS addition (gray) and after 4 days (blue).

Next, the dispersion stability of the QA nanoparticles prepared in water and the BSA solution was evaluated in PBS, physiologically relevant conditions. Figure 3(a) shows the changes in the absorption spectra of QA nanoparticles prepared in water after PBS addition. The decrease in the absorbance immediately after PBS addition is partially due to dilution. Simultaneously, the mean particle size became 1053 nm.

After 4 days, a noticeable decrease in absorbance was observed. The mean particle size became 3155 nm with PDI of 1.20, as seen in Fig. 3(b). This decreased absorbance was recovered through sonication by about 80% of immediately after PBS addition. These results indicated that the QA nanoparticles were agglomerated in PBS although the mean particle size did not return to the initial state, remaining at 677 nm with PDI of 0.54.

The zeta potential of the QA nanoparticles in water was determined to be approximately -50 mV; this high surface charge is responsible for maintaining their stability in the aqueous medium. Consequently, it is considered that the nanoparticles lose this protective surface charge upon introduction to PBS: highly ionic conditions, thereby triggering agglomeration.

In contrast, QA nanoparticles prepared in the BSA solution exhibited minimal changes in their absorption spectrum following PBS addition, as illustrated in Fig. 4(a). The mean particle size increased to 146 nm with a PDI of 0.17 and to 140 nm with a PDI of 0.28 after PBS addition and 4 days later respectively, indicating that the nanoparticles remained stably dispersed over time in PBS.

These findings suggest that BSA adsorbs efficiently onto the nanoparticle surface, thereby suppressing agglomeration. While electrostatic interactions often contribute to protein adsorption, high salt concentrations tend to screen these charges and weaken the binding. In this study, the stability maintained under ionic conditions suggests that the adsorption is primarily driven by hydrophobic interactions.

BSA is known to possess multiple hydrophobic pockets, which facilitate strong binding to various hydrophobic surfaces [11]. This hydrophobic anchoring creates a robust steric barrier that prevents nanoparticle aggregation even in high-ionic-strength environments [12].

Finally, fluorescence spectra were measured to elucidate the effect of BSA adsorption on the nanoparticle surface (Fig. 5a). In general, the fluorescence properties of organic fluorophores are sensitive to changes in the local environment [13]. When BSA adsorbs onto the nanoparticle surface, it alters the surrounding environment from an aqueous phase to a more hydrophobic environment. This might lead to changes in fluorescence spectrum, providing indirect evidence of the interaction between BSA and the nanoparticles. In pure water, QA exhibited a broad emission spectrum ranging from 550 to 750 nm, characteristic of the solid-state fluorescence of QA crystals. The sharp band observed around 560 nm is attributed to the Raman scattering of water and is therefore disregarded in this analysis. Following laser irradiation in water, only a slight increase in fluorescence intensity was observed due to the increased absorbance (i.e., increased number of particles).

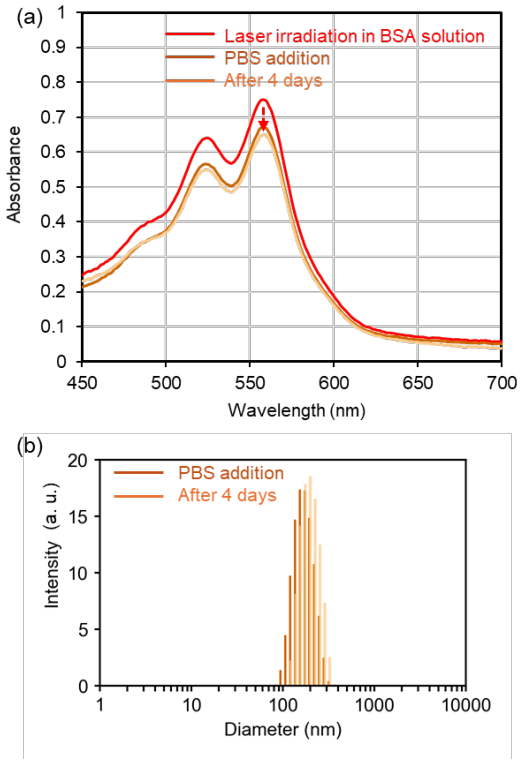

Fig. 4 (a) UV-vis absorption spectra of QA nanoparticles formed in BSA solution (red) and immediately after PBS addition (brown) and after 4 days (orange). (b) Particle size distributions of QA nanoparticles after PBS addition (brown) and after 4 days (orange).

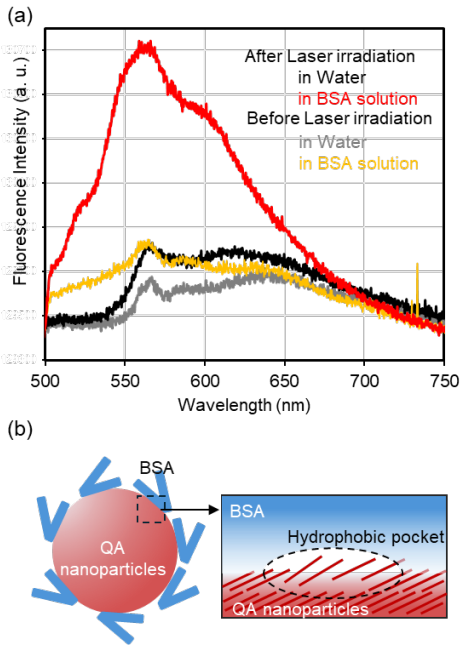

Fig. 5 (a) Fluorescence spectra of QA suspended before laser irradiation in water (gray) and in BSA solution (orange) and after laser irradiation in water (black) and in BSA solution (red). (b) Schematic illustration of BSA adsorption on the nanoparticle surface and its possible effect on surface molecular stacking.

In contrast, the presence of BSA significantly modified the fluorescence spectra. Even before irradiation, the spectrum showed structural features of QA dissolved in DMSO [14]. This molecular-like fluorescence signal was further enhanced after laser irradiation.

Adsorption of BSA via hydrophobic interactions would perturb the π-π molecular stacking at the particle-water interface, creating a microenvironment where surface molecules behave more like monomers (Fig. 5b). Consequently, the fluorescence spectrum shifts from a solid-state emission to a molecular-like emission. The significant reduction in particle size increases the specific surface area, which facilitates the adsorption of BSA. This BSA-induced disturbance of the surface molecular arrangement likely reduces the interfacial surface tension, which may also explain the enhanced fragmentation efficiency (smaller mean particle size) observed in the BSA solution compared to pure water.

Previously, we reported that the presence of BSA improved the stability of PR149 nanoparticles in PBS. However, unlike the current findings with QA, PR149 did not exhibit either enhanced fragmentation efficiency or modifications in its fluorescence properties. This discrepancy indicates that the influence of BSA varies significantly depending on the specific organic compound.

As noted in the introduction, QA possesses a lower tPSA compared to PR149, reflecting its higher hydrophobicity. Since the interactions between the nanoparticle surface and BSA are predominantly governed by hydrophobic interactions, we conclude that QA undergoes stronger interactions with BSA.

4. Conclusion

This study demonstrated that BSA serves as a biocompatible dispersing agent for the fabrication of QA nanoparticles by PLFL. Unlike PR149, which only showed improved colloidal stability with BSA, QA exhibited both enhanced fragmentation efficiency and distinct modifications in fluorescence properties. These differences could be attributed to the lower tPSA and higher hydrophobicity of QA, which facilitate stronger hydrophobic interactions between the nanoparticle surface and BSA molecules. This interaction not only provides steric hindrance against salt-induced agglomeration in physiological environments but also perturbs the surface crystalline order of the nanoparticles.

While this study focused on the contrast between QA and PR149, further systematic investigations involving a broader range of tPSA values and other physicochemical properties, such as the octanol-water partition coefficient, will be necessary to fully understand the impact of this effect. Nevertheless, our findings reinforce the potential of BSA as a versatile additive for the laser-based production of nanopharmaceuticals, especially for highly hydrophobic candidates.

References

[1] H. D. Williams, N. L. Trevaskis, S. A. Charman, R. M. Shanker, W. N. Charman, C. W. Pouton, and C. J. H. Porter: Pharmacol. Rev., 65, (2013) 315. (Journals)
[2] B. Xie, Y. Liu, X. Li, P. Yang, and W. He: Acta Pharm. Sin. B, 14, (2024) 4683. (Journals)

[3] M. Haripriyaa and K. Suthindhiran: Future J. Pharm. Sci., 9, (2023) 69. (Journals)
[4] G. Pasut, Front. Med.: Technol., 1, (2019), 1. (Journals)
[5] K. Yuyama, T. Sugiyama, T. Asahi, S. Ryo, I. Oh, and H. Masuhara: Appl. Phys. A, 101, (2010) 591. (Journals)
[6] R. Yasukuni, M. Sliwa, J. Hofkens, F. C. De Schryver, A. Herrmann, K. Müllen, T Asahi: Jpn. J. Appl. Phys, 48, (2009), 065002. (Journals)
[7] T. Friedenauer, M. Spellauge, A. Sommereyns, C. Rehbock, H. P. Huber, S. Barcikowski: J. Phys. Chem. C, 129, (2025) 6803. (Journals)
[8] R. Yasukuni, A. Sunada, N. Fujiwara, N. Masuda, Y. Atsuta, S. Fujii, and T. Kamimura: Commun. J. Photopolym. Sci. Technol., 37, (2024) 401. (Journals)
[9] D. F. Veber, S. R. Johnson, H-Y. Cheng, B. R. Smith, K. W. Ward and K. D. Kopple: J. Med. Chem. 45, (2002) 2615. (Journal)
[10] T. Sugiyama, T. Asahi, H. Takeuchi, and H. Masuhara: Jpn. J. Appl. Phys., 45, (2006) 384. (Journals)
[11] B. A. Russell, K. Kubiak-Ossowska, P. A. Mulheran, D. J. S. Birch, and Y. Chen: Phys. Chem. Chem. Phys., 17, (2015) 21935. (Journals)
[12] R. Zhong, Y. Liu, P. Zhang, J. Liu, G. Zhao, and. Zhang: ACS Appl. Mater. Interfaces, 6, (2014) 19465. (Journals)
[13] A. Jain, E. Judy, and N. Kishore: J. Phys. Chem. B, 128, (2024), 5344. (Journals)
[14] E. Rossin, Y. Yang, M. Chirico, G. Rossi, P. Galloni, and A. Sartorel: Energy Adv., 3, (2024), 1894. (Journals)

(Received: February 9, 2026, Accepted: May 16, 2026)